

Nucleation, Growth, and Aggregation of Ag Clusters on Liquid Surfaces

Gao-Xiang Ye,^{1,2} Thomas Michely,^{1,*} Volker Weidenhof,¹ Inés Friedrich,¹ and Matthias Wuttig^{1,†}

¹*Institut für Grenzflächenforschung und Vakuumphysik, Forschungszentrum Jülich, D-52425 Jülich, Germany*

²*Department of Physics, Hangzhou University, Hangzhou 310028, People's Republic of China*

(Received 16 December 1997; revised manuscript received 12 May 1998)

We report the formation of large, branched silver aggregates after deposition of Ag on silicone oil surfaces. The origin of these ramified aggregates is traced to a two stage process, the first of which involves nucleation and growth of disk-shaped Ag clusters during deposition. In the subsequent stage after deposition, the clusters continue to diffuse on the liquid surface by Brownian motion and finally aggregate. [S0031-9007(98)06633-2]

PACS numbers: 68.10.-m, 68.35.Fx, 81.15.Tv

In this Letter, we present results on the growth of Ag on silicone oil surfaces in the limit of low coverage, i.e., below a few monolayers [1]. The most exciting and unexpected result is visualized in Fig. 1, where it can be seen that the deposited Ag forms branched aggregates on the oil surface. Branch thicknesses up to a few microns and total dimensions of several tens of microns are observed. The processes leading to these “fractal” aggregates appear complex. Nevertheless, their shapes resemble the results of computer models for diffusion limited aggregation (DLA) [2] of particles or even more closely to those of cluster-cluster aggregation (CCA) [3] in two dimensions. In this Letter, we will demonstrate that the formation mechanisms of these structures can be understood with the aid of experiments comparing different growth rates and film thicknesses as well as by comparison to models for growth, diffusion, and aggregation [2–5].

In order to prepare flat liquid surfaces of well defined thickness, silicone oil with a low vapor pressure [6] was spin coated at 6000 rpm onto 1 cm² transparent plastic slides. The edges of the polycarbonate slides were slightly roughened to prevent the oil layers from dewetting the smooth plastic surface. The resulting oil films had a uniform thickness of $\approx 10 \mu\text{m}$. Silver 99.999% pure was deposited by thermal evaporation in a vacuum of 2×10^{-6} mbar at room temperature ($23 \pm 4^\circ\text{C}$). The deposition rate was varied from 0.01 to 0.20 nm/s. The nominal film thickness deposited was 0.15 nm in all measurements shown here except for those shown below in Fig. 3(a). The film thickness was determined by a quartz-crystal balance located near the substrate. The quartz-crystal balance was calibrated by atomic force microscopy and x-ray reflectometry for thick deposited films. After deposition, the samples were removed from the evaporation chamber. The Ag/oil surface was characterized under ambient conditions with an optical microscope mounted on a vibration isolation table. The first images were taken between 30 minutes and 1 hour after deposition. Subsequently, the evolution of the film structure with time was followed up to one week. From the apparent Ag cover-

age of 10%–20% of the total area, and the nominal deposited film thickness of 0.15 nm, we conclude that the Ag forms flat platelets with thicknesses between three and seven atomic layers. From the cluster sizes, we get that a platelet contains of the order of 10^8 Ag atoms. X-ray diffraction scans of thick films (≈ 30 nm) grown on the oil surface give evidence for a film texture with a preferential (111) orientation. One may therefore assume that the flat faces of the thin Ag clusters also expose (111) planes. By moving the focal plane of the microscope objective through the oil film, it is found that the Ag clusters are located at the oil surface or, more precisely, not farther than $0.2 \mu\text{m}$ away from the top surface.

To unravel the different processes occurring during and after Ag deposition, a series of experiments was performed in which the deposition rate was varied between 0.01 and 0.20 nm/s. We then followed the evolution of the Ag/oil surface morphology over time. Figure 2 compares the results for two different deposition rates. Using a low deposition rate of 0.03 nm/s, the first image taken

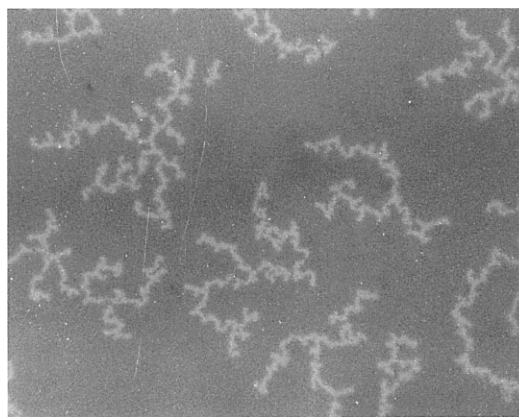


FIG. 1. Ag aggregates on silicone oil formed by exposure to Ag vapor from a thermal Ag evaporator. 0.15 nm of Ag is deposited with a deposition rate of 0.2 nm/s. The image is taken through an optical microscope 18 h after deposition and has a size of $73 \times 57 \mu\text{m}^2$. The branch thickness of the aggregates is about $0.7 \mu\text{m}$, and their typical lateral dimension (diameter of containing circle) is $25 \mu\text{m}$.

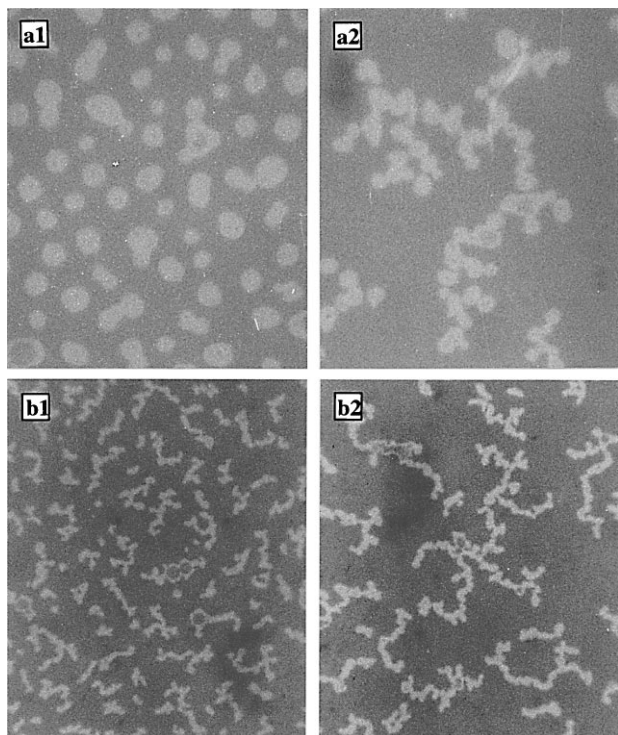


FIG. 2. Deposition rate and time dependence of the morphology. In (a1) and (a2) the deposition rate was 0.03 nm/s, and in (b1) and (b2) it was 0.1 nm/s. (a1) and (a2) were taken 1 and 30 h after deposition, respectively, and (b1) and (b2) 1 and 3 h after deposition, respectively. Image size is $50 \times 42 \mu\text{m}^2$.

1 h after deposition exhibits only compact Ag clusters with a typical diameter of $2.5 \mu\text{m}$ [Fig. 2(a1)]. However, over the course of time, we find that the single clusters move in a random fashion with respect to each other. When two clusters touch, they irreversibly adhere to each other and from then on move as one unit. These units do not coalesce into a more compact shape. Only very few events were observed, for which two clusters separated again after they adhered. After 30 h, all single compact clusters are aggregated to large branched islands [Fig. 2(a2)]. These structures resemble the ramified aggregates shown in Fig. 1, but are larger in size and branch thickness. In the large aggregate of Fig. 2(a2), the individual clusters from which the branched chains are composed can still be discerned. In the case of a sample deposited using a high deposition rate of 0.10 nm/s, the image taken after 1 h [Fig. 2(b1)] already exhibits branched aggregates with a typical branch thickness of about $1.0 \mu\text{m}$. Nonetheless, these aggregates still perform random motion, and if two of them touch, they adhere to each other and form an even larger aggregate. The situation 3 h after deposition is shown in Fig. 2(b2). Again large ramified aggregates similar to Fig. 1 result.

Based on these observations, we suggest a two stage description of aggregate formation. Schematically, it

may be subdivided into growth of disk-shaped clusters during deposition (stage-I) and subsequent aggregation of clusters (stage-II). We assume for both stages that silver atoms, clusters of various sizes, and aggregates of clusters all migrate on the oil surface by a random walk motion, due to statistical fluctuations in their momentum by collisions with liquid molecules. Their mean square displacement $\langle \Delta r^2 \rangle$ is given by $\langle \Delta r^2 \rangle = 4kTF^{-1}\Delta t$ for a two dimensional motion according to the theory of Brownian motion [7], where k is the Boltzmann constant, T is the temperature, Δt is the time, and F is the friction coefficient. The friction coefficient F will be a function of the size and shape of the aggregates and is expected to increase with the number of particles in the object. It is related to the diffusion coefficient D by $D = kTF^{-1}$.

In order to discuss stage-I, we define a stable cluster as one that more probably grows than shrinks [8]. In the present case of cluster size dependent mobility the stability of a cluster implies (i) that the rate of material dissociation from the cluster is smaller than the rate of material incorporation and (ii) that the probability of the mobile cluster to become incorporated into an even larger cluster is negligible. At the beginning of stage-I, because of deposition the concentration of Ag atoms increases with time. These atoms migrate rapidly over the liquid surface forming small Ag clusters upon encounter. Subsequently, larger, slower, and stable Ag clusters are formed at the expense of mobile Ag atoms and small, unstable Ag clusters. The deposition rate sets the time and thereby the distance available for diffusion of small atoms and unstable clusters. Thus the number density of stable clusters will increase with deposition rate. The stable clusters efficiently deplete their surroundings of adatoms and small clusters and hence, after a short nucleation phase, *no more stable clusters are formed*. As the diffusion of large clusters is slow, the encounter of two stable clusters is a rare event and the number density of stable clusters remains almost constant during their subsequent growth (i.e., saturates). As the stable clusters communicate via their diffusion fields and grow for similar times from nucleation until the end of deposition, at this time a relatively narrow size distribution of clusters is expected. The growing clusters do not develop branches during growth since Ag surface self-diffusion is efficient at room temperature [9]. The scenario presented here corresponds largely to classical nucleation theory in epitaxy with the additional assumption of cluster size dependent mobility as in the deposition, diffusion, and aggregation (DDA) model [5,10].

Stage-II starts at the end of deposition and implies a switch in time scales. While stage-I is completed after a few seconds, those changes in the island density, size, and shape, which are characteristic for stage-II, are observed on a time scale of hours or even days. On this time scale, the Brownian motion of the compact clusters formed during deposition is no longer negligible, and

mean square displacements of the order of μm occur. The large clusters migrate, and if two clusters touch they adhere to each other. They do not coalesce because either the surface material transport is too small on this size scale or an adsorbed layer of oil molecules around the individual clusters prevents direct contact. The scenario we assume for stage-II corresponds largely to the cluster-cluster aggregation model [3] with the ingredients of an initial distribution of similar sized clusters performing Brownian motion, which adhere upon impact.

Given the above two stage description, the dependence of the fractal appearance upon deposition rate in Figs. 2(a1) and 2(b1) can be explained. For low deposition rates, a small number density of large clusters results. Since the motion of the correspondingly large clusters is slow, at the moment of our first observation, they are still compact clusters—relatively unchanged from their appearance at the end of deposition [Fig. 2(a1)]. It is only after about 10 hours that the aggregation has considerably proceeded and fractals are formed [Fig. 2(a2)]. In contrast, for high deposition rates, the small compact clusters present at the end of deposition have a much higher mobility. Consequently, at the moment of our first observation, 1 h after deposition, they are already aggregated [Fig. 2(b1)] and subsequently we only observe the assembly of these aggregates to even larger fractals [Fig. 2(b2)].

If the description of stage-I is correct, we expect the cluster number density to saturate at a certain deposited amount, as in the corresponding theoretical models [4,5]. We measured the cluster number density as a function of film thickness for a deposition rate of 0.03 nm/s [Fig. 3(a)] [11]. Indeed, the cluster number density exhibits a broad saturation maximum between 0.06 and 0.3 nm deposited. At 0.45 nm we already observe percolation. Nucleation theory [4] and the DDA model [5] both predict scaling of the saturated cluster density N_x with the deposition rate f of the form of $N_x \propto f^\chi$, at least as long as the friction coefficient F scales to some power with cluster size. Unfortunately, we are unable to measure the cluster number density precisely at the end of deposition for a wide range of deposition rates. Therefore we analyzed the average branch thickness d of the aggregates, which we assume in good approximation to be identical to the average cluster diameter d : $N_x \propto \frac{\Theta_{\text{sat}}}{d^2}$ for a fixed coverage Θ_{sat} . Our results are displayed in the log-log plot in Fig. 3(b). Indeed, the branch thickness scales with the deposition flux as $d \propto f^{-0.69 \pm 0.05}$, which gives rise to an exponent $\chi = 1.38 \pm 0.10$. This value is unexpectedly large in view of the fact that in nucleation theory χ just approaches 1 in the case of large unstable cluster sizes. However, including diffusion of the clusters as in the DDA model leads to a significant increase in χ [5].

If the description of stage-II is correct, Brownian motion of the clusters on the liquid surface is expected. This is consistent with the results shown graphically in Fig. 4(a), where for the two cluster groups represented

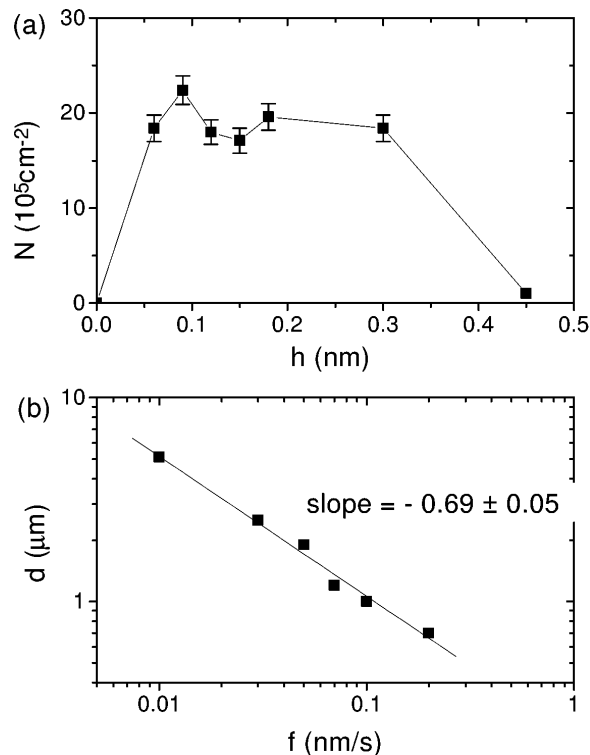


FIG. 3. (a) Cluster density N measured 1.5 h after deposition as a function of the deposited amount, expressed as nominal film thickness h . Deposition rate 0.03 nm/s. Lines connect the data points. (b) Average branch thickness d of cluster aggregates vs deposition rate f . The solid line is a linear fit to the data.

the relative mean square displacement $\langle \Delta r^2 \rangle$ between two clusters increases linearly with time. The resulting diffusion coefficients are of the order of $10^{-11} \text{ cm}^2/\text{s}$. The cluster group with the larger total area [see Fig. 4(a)] has the smaller diffusion coefficient, in line with our assumption of a size dependent friction coefficient. For Brownian motion of spherical clusters consisting of n atoms in a liquid, according to Stoke's law, a friction coefficient $F \propto n^{1/3}$ is expected. For Brownian motion of platelets on a surface with the friction proportional to the contact area, one expects $F \propto n^1$. We measured the friction coefficient of the clusters over little more than an order of magnitude in size, in the size range of $n \approx 10^8 - 10^9$ atoms per aggregate. As expected the friction coefficient F increases with increasing cluster size and the overall friction coefficient is about 0.6. However, the data are not unambiguous, and it appears that there is not a uniform friction exponent. A clear dependence of the friction on the cluster shape is found. The friction of a branched cluster aggregate is larger than the one of a compact cluster with the same size.

Clusters and cluster aggregates do not perform only random lateral motion. As soon as their shape deviates significantly from a disk, another kind of lateral motion becomes apparent. Clusters and cluster aggregates also

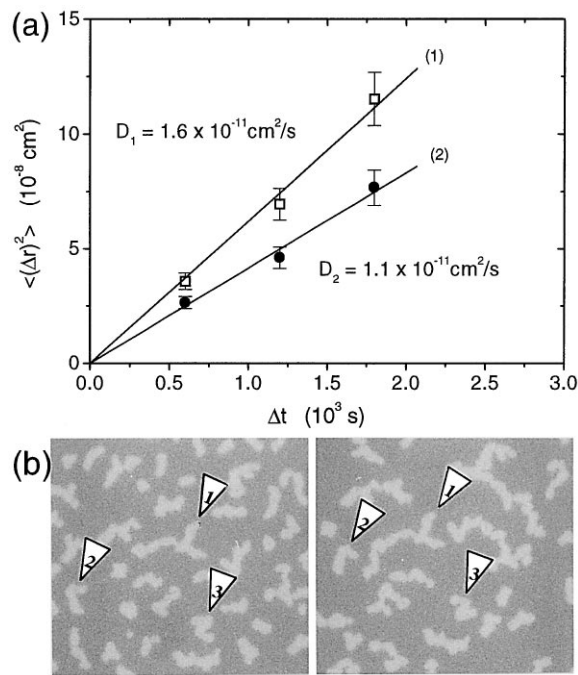


FIG. 4. (a) Relative mean square displacement $\langle (\Delta r)^2 \rangle$ between two clusters as a function of time. Total area of the two clusters is $3.6 \mu\text{m}^2$ (squares) and $8.3 \mu\text{m}^2$ (dots). (b) Rotation of cluster aggregates is apparent by comparison of the positions of the aggregates 1, 2, and 3 in the left and right topograph taken 1.5 h apart ($36 \times 33 \mu\text{m}^2$).

perform random rotational motion with the mean square angular displacement $\langle \Delta \Phi^2 \rangle$ per time interval decreasing with increasing cluster size. In Fig. 4(b), two successive images ($\Delta t = 1.5 \text{ h}$) are shown with 3 clusters marked which perform random rotations.

Finally, we analyzed the scaling properties of the aggregates resulting at the end of stage-II. The aggregates resulting for deposited amounts of 0.15 nm exhibit a fixed fractal dimension over more than 1 order of magnitude in length scale. Depending on statistics, details of image analysis and deposition condition, we obtain with the box counting method fractal dimensions between 1.3 and 1.5. As an example, for the aggregates resulting from the run of Fig. 1 the fractal dimension is 1.37 ± 0.04 . The dimension obtained is inconsistent with a DLA model ($5/3$ expected) [2], but agrees well with the ones for cluster-cluster aggregation models which are in the range of 1.32–1.50 [3]. This agreement lends strong support to our description of the stage-II of aggregate formation. We note that the fractal dimensions determined for similar shaped aggregates resulting from atom [12] or cluster [13] deposition on solid substrates were always higher (1.50–1.90) than the ones obtained for the Ag aggregates resulting from deposition on the liquid oil surface. The lower fractal dimension obtained on the liquid substrate is consistent with the comparatively less branched appearance of the Ag aggregates on oil. The

different fractal dimensions for the two classes of systems are most likely due to the fact that motion of atom or cluster aggregates is absent on solid substrates, while Brownian motion for cluster aggregates is also present on the liquid surface.

We thank Bernd Schirmer, Josef Larscheid, Marc Henke, Han-Willem Wöltgens, and Sun-Joung You for useful discussions and technical assistance. G. X. Y. gratefully acknowledges the hospitality of the Institut für Grenzflächenforschung und Vakuumphysik and the support by the Pao Yu-kong and Pao Zhao-long Scholarship of China. Th. M. and M. W. acknowledge support by the Deutsche Forschungsgemeinschaft.

*Corresponding author.

Present address: I. Physikalisches Institut, RWTH Aachen, D-52056 Aachen, Germany.

Electronic address: michely@physik.rwth-aachen.de

†Permanent address: I. Physikalisches Institut, RWTH Aachen, D-52056 Aachen, Germany.

- [1] Previous work showed that continuous Ag films are formed on silicone oil surfaces, if sufficient quantities of the metal are sputter deposited. See G. X. Ye, Q. R. Zhang, C. M. Feng, H. L. Ge, and Z. K. Jiao, *Phys. Rev. B* **54**, 14 754 (1996).
- [2] T. A. Witten, Jr. and L. M. Sander, *Phys. Rev. Lett.* **47**, 1400 (1981).
- [3] M. Kolb, R. Botet, and R. Julien, *Phys. Rev. Lett.* **51**, 1123 (1983); P. Meakin, *Phys. Rev. Lett.* **51**, 1119 (1983).
- [4] J. A. Venables, G. D. T. Spiller, and M. Hanbücken, *Rep. Prog. Phys.* **47**, 399 (1984).
- [5] P. Jensen, A. L. Barabasi, H. Larralde, S. Havlin, and H. E. Stanley, *Phys. Rev. B* **50**, 15 316 (1994).
- [6] Dow Corning 705 Diffusion Pump Fluid.
- [7] A. Einstein, *Ann. Phys. (Leipzig)* **17**, 549 (1905); **19**, 371 (1906); Ira N. Levine, *Physical Chemistry* (McGraw-Hill, New York, 1988).
- [8] D. Walton, *J. Chem. Phys.* **37**, 2182 (1962).
- [9] J. M. Wen, S. L. Chang, J. W. Burnett, J. W. Evans, and P. A. Thiel, *Phys. Rev. Lett.* **73**, 2591 (1994).
- [10] The DDA model differs from the present situation, as here (i) the growing clusters are kept compact by diffusion at the cluster surface and (ii) there is no reason to assume atom dissociation from a cluster to be negligible.
- [11] For the low rate of 0.03 nm/s the cluster density changes only marginally between the end of deposition and the first imaging 1.5 h later.
- [12] R. Q. Hwang, J. Schröder, C. Günther, and R. J. Behm, *Phys. Rev. Lett.* **67**, 3279 (1991); Th. Michely, M. Hohage, M. Bott, and G. Comsa, *Phys. Rev. Lett.* **70**, 3943 (1993); H. Brune, C. Romainczyk, H. Röder, and K. Kern, *Nature (London)* **369**, 469 (1994).
- [13] L. Bardotti, P. Jensen, A. Hoareau, M. Treilleux, and B. Cabaud, *Phys. Rev. Lett.* **74**, 4694 (1995); L. Bardotti, P. Jensen, A. Hoareau, M. Treilleux, B. Cabaud, A. Perez, and F. C. S. Aires, *Surf. Sci.* **367**, 276 (1996).